Production of ozone and nitrogen oxides by laser filamentation

Yannick Petit, Stefano Henin, Jérôme Kasparian,[a] and Jean-Pierre Wolf
GAP Biophotonics, Université de Genève, 20 rue de l'École de Médecine, CH1211 Genève 4, Switzerland

(Received 4 June 2010; accepted 21 June 2010; published online 15 July 2010)

We have experimentally measured that laser filaments in air generate up to 10^{14}, 3×10^{12}, and 3×10^{13} molecules of O_3, NO, and NO_2, respectively. The corresponding local concentrations in the filament active volume are 10^{16}, 3×10^{14}, and 3×10^{15} cm^{-3}, and allows efficient oxidative chemistry of nitrogen, resulting in concentrations of HNO_3 in the parts per million range. The latter forming binary clusters with water, our results provide a plausible pathway for the efficient nucleation recently observed in laser filaments. © *2010 American Institute of Physics*.
[doi:10.1063/1.3462937]

In their propagation through transparent media, ultrashort laser pulses can generate self-guided filaments.[1–4] Filamentation stems from a dynamic balance between Kerr self-focusing on one side, and defocusing by both higher-order (negative) Kerr terms,[5] and the free electrons originating from the ionization of the propagation medium by the pulse itself. Filaments, which can be longer than 100 m,[6] be initiated remotely[7] and propagate through clouds[8] and turbulence,[9] are ideally suited for atmospheric applications[4,10] like lightning control,[11] or laser-assisted water nucleation.[12]

In subsaturated atmospheres, the latter effect cannot be explained by the Wilson mechanism[13] in which the charges stabilize charge-transfer complexes of $H_2O^+O_2^-$, on which droplets grow. Rather, the observed effect may imply binary nucleation of HNO_3,[14–16] which according to the extended Köhler theory stabilizes the growing droplets of binary mixtures, similar to observations in cloud chambers for binary H_2SO_4–H_2O.[17,18] Assessing this pathway requires a precise knowledge of the physicochemistry of the filaments. In this paper, we measure the generation of three key gases, namely O_3, NO, and NO_2 by laser filaments. Filaments produce large amounts of these trace gases, allowing efficient oxidative chemistry of nitrogen and resulting in concentrations of HNO_3 in the multiparts per million range, which may account for the efficient droplet nucleation induced by laser filaments in sub-saturated atmospheres.[12]

The experiments (Fig. 1) were conducted on the Helvetera platform, which delivered laser pulses of up to 12 mJ energy and 80 fs Fourier-limited duration (150 GW peak power) at a wavelength of 800 nm and 100 Hz repetition rate. A chopper reduced this rate by a factor of 40 in most experiments (i.e., an average of 2.5 pulses/s) to limit the concentration in the cell and reduce the chemical reactions between the generated species as well as to avoid saturation of the measurement devices. The incident pulse duration was varied by detuning the laser compressor to induce a chirp. The beam (2×2.4 cm cross section) was focused by an $f=2.8$ m lens to generate one to two filaments in a 2 m long Plexiglas cell of 2 cm diameter with 250 μm thin fused silica windows. Fresh air from the room entered freely the cell at one of its ends. At its other end, the air was continuously pumped in parallel through polyethylene tubes by an ozone analyzer (Horiba APOA-350E) at a flow of 2.2 l/min and a NOx analyzer (Monitor laboratories 8840) at a flow of 0.5 l/min. Although in the filaments, ozone and NOx are partly ionized, the transit time of ~10 s through the sampling circuit ensures that they are neutralized before entering the analyzers, so that ionized species are measured together with neutral ones.

All measurements were performed once steady state was reached in the cell. We checked that all measurements were linear with the number of laser shots per unit time. If we neglect chemical reactions among the NOx and O_3 during the transit to the analyzers, the variation in the measured concentration C_i of species i depends on the generation of this species by the laser beam (source term S_i) and its dilution by the flow F through the cell.

$$V\times dC_i/dt = S_i - F\times C_i. \tag{1}$$

In a steady state, the source term reads the following:

$$S_i = C_i \times F. \tag{2}$$

Volumic generation rates and the resulting concentrations are then evaluated by dividing S_i by the total filament volume, corresponding to two filaments of 0.5 m length and of 100 μm diameter, i.e., a total volume of 4 mm^3. In Eqs. (1) and (2), we have neglected the losses and source terms due to chemical reactions, especially the oxidation of NO and NO_2 by ozone[17]

$$NO + O_3 \rightarrow NO_2 + O_2, \tag{3}$$

$$NO_2 + O_3 \rightarrow NO_3 + O_2, \tag{4}$$

as well as on the walls of the cell, mainly the degradation of ozone into O_2 on the wall surface, as follows:

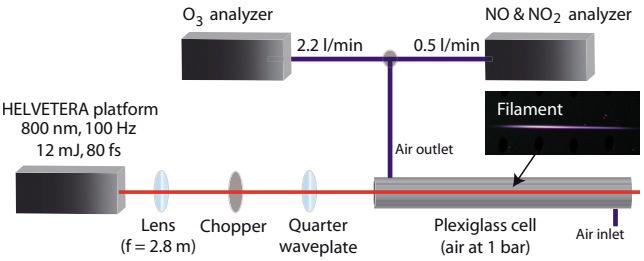

FIG. 1. (Color online) Experimental setup.

[a]Electronic mail: jerome.kasparian@unige.ch.

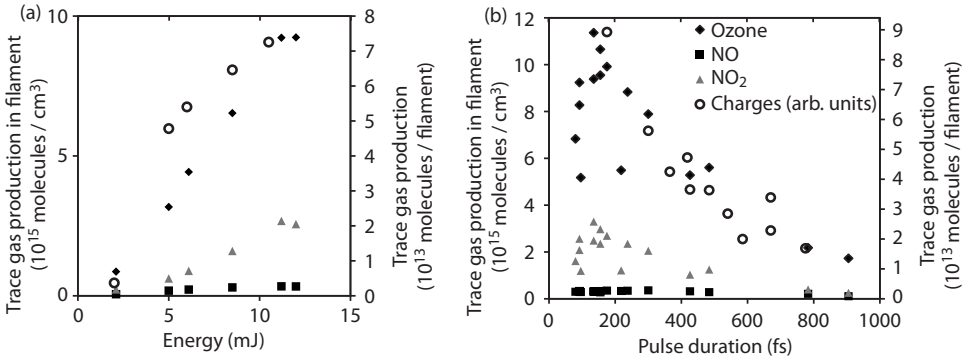

FIG. 2. Generation of O_3, NO, and NO_2 in laser filaments as a function of (a) the incident energy for a pulse duration of 80 fs and (b) the pulse duration for a pulse of 11.2 mJ energy.

$$2O_3 \rightarrow 3O_2. \quad (5)$$

We, therefore, measure a lower limit for the production of O_3 and NO by the laser filaments. On the other hand, the effect on NO_2 is more complex, since Reactions (3) and (4) have opposite effects. These contributions are discussed at the end of the present manuscript. In parallel with the concentration of trace gases, we measured the relative efficiency of charge release by the filaments, as detailed in Ref. 19.

Figure 2 displays the generation rate per unit volume of O_3, NO, and NO_2 in the filament as a function of the incoming pulse energy and duration. Obviously, the filaments produce considerable amounts of these trace gases. For 2.5 shots/s, the concentrations averaged over the cell volume reach 200 ppb of O_3 and 50 ppb of NO_2, one order of magnitude above typical atmospheric values and even higher than the alert level in most countries. They correspond to the generation of extremely high concentrations within the filament volume: 400 ppm (10^{16} cm^{-3}) of ozone and 100 ppm of NO_2 (3×10^{14} cm^{-3}), respectively.

The production of O_3, NO, and NO_2 increases quite linearly with pulse energy, with a threshold between 1 and 2 mJ, corresponding to the filamentation threshold in our experimental conditions. It is proportional to that of electrons for various pulse durations and energies (Fig. 2). Linearly polarized pulses yield 19% more ozone, 33% more NO, and 68% more NO_2, consistent with the fact that a linear polarization is more favorable to filamentation than a circular one,[20] resulting, in our setup, in twice as much charge generation than circularly polarized pulses. These data show that NOx and ozone are mainly produced in the filaments, hence in plasma, rather than in the photon bath. The corresponding pathways may therefore be activated by photodissociation, ionization, or electron impact onto O_2 and N_2 molecules. The very complex chemistry occurring in air plasmas[21,22] prevents us to isolate one single scheme, although three of them are more likely to contribute significantly to the formation of NO. The first one relies on the N^+ ions, which are highly reactive with O_2, with a rate constant as high as 5×10^{-10} cm^3/s at 300 K. Note that, throughout this work, we use of the rate constants at room temperature because the filaments are known to negligibly heat the heavy species of the plasma.[2,3] The branching ratios are 43%, 51%, and 6% between the reactions, as follows[23]:

$$N^+ + O_2 \rightarrow NO^+ + O^\bullet, \quad (6)$$

$$N^+ + O_2 \rightarrow N + O_2^+, \quad (7)$$

$$N^+ + O_2 \rightarrow NO + O^+. \quad (8)$$

Alternatively, the recombination of electrons with N_2^+, can break the N–N bond and lead to the following[24]:

$$e + N_2^+ \rightarrow N^* + N. \quad (9)$$

The excited nitrogen atom can also be generated by the following[21]:

$$N_2^* + O^\bullet \rightarrow NO + N^*. \quad (10)$$

The activated nitrogen atoms will then react with oxygen molecules, as follows:

$$N^* + O_2 \rightarrow NO + O^\bullet. \quad (11)$$

Besides Reactions (6) and (11), $O^\bullet$ is also produced by the following[25]

$$e + O_2 \rightarrow O^\bullet + O^\bullet. \quad (12)$$

The oxygen atoms immediately react with oxygen molecules, as follows:

$$O^\bullet + O_2 + M \rightarrow O_3 + M. \quad (13)$$

Ozone will then oxidize NO into NO_2 through reaction (3). Although the main reaction paths are identified above, simulations of the measured concentrations using rate equations is currently impossible because of the very riche chemical dynamics at play[21] and of the lack of data on the initial N^*, N_2^*, N^+, and N_2^+ concentrations in the filaments. However, since the concentration of O_3, NO, and NO_2 are closely related to that of the electrons, a process initiation by Reactions (6)–(9) is more likely than (10). The very high concentrations O_3 and NO_2 in the filament volume allow an efficient chemistry. In particular, the equilibrium[17]

$$NO_2 + NO_3 + M \rightleftarrows N_2O_5 + M, \quad (14)$$

is governed by $K_{14}=[N_2O_5]/([NO_2][NO_3])=3\times10^{-11}$ cm^3 at 298 K. N_2O_5 immediately reacts with water, as follows:

$$N_2O_5 + H_2O(s) \rightarrow 2HNO_3. \quad (15)$$

Given the rate constant $k_4=3\times10^{-17}$ cm^3/s of Reaction (4),[17] the extremely high NO_2 and ozone concentrations in the filaments could generate up to 6×10^{14} molecules/cm^3/s of NO_3, a production rate comparable with that of NO_2 in our experiments. Considering the equilibrium constant K_{14} and the reaction rate $k_{15}=3\times10^{-4}$ s^{-1}, Reactions (4), (14), and (15) clearly result in the generation of N_2O_5, hence HNO_3, in the parts per million range, or even higher. Binary HNO_3–H_2O clusters[16] then form, grow into condensation nuclei and allow macroscopic

droplet formation and net uptake of water from the atmosphere. Reactions (6)–(15) provide a large excess of condensation nuclei as compared with the droplet densities of at most some 10^3 cm^{-3} observed in our recent nucleation experiments.[12] Chemistry therefore appears as the dominant process in laser-induced condensation in subsaturated atmospheres. At least, that relevant species are is available in amounts largely sufficient to explain the observed condensation.

Up to now, we have neglected the losses due to Reactions (3)–(5). Since all species are generated simultaneously, their concentrations can be considered as roughly proportional (as is also visible on Fig. 2) so that the reaction rates depend on the square of the considered concentration. Under this assumption, the rate Eq. (1) rewrites, for each species i, as follows:

$$V \times dC_i/dt = S_i - k_i C_i^2 - FC_i, \tag{16}$$

so that in the steady state,

$$C_i = (-F + \sqrt{F^2 + 4k_i S_i})/2k_i. \tag{17}$$

Comparing results in two conditions with identical source term and different pumping rates (hence, sampling flows) yields

$$k_i = (C_{i,1}F_1 - C_{i,2}F_2)/(C_{i,2}^2 - C_{i,1}^2). \tag{18}$$

In the case of ozone, we measured $[O_3]_1 = 314$ ppb for $F_1 = 2.2$ l/min and $[O_3]_2 = 285$ ppb for $F_2 = 2.7$ l/min, which yields $k_{O_3} = 4.5$ l/min/ppm. Implementing this correction increases the source term by at most 10%: the losses due to ozone depletion via chemical processes in the flow cell is not the main source of error. Furthermore, $[NO_2]_1 = 124$ ppb for $F_1 = 0.5$ l/min and $[NO_2]_2 = 32$ ppb for $F_2 = 2.7$ l/min, result in $k_{NO_2} = 1.7$ l/min/ppm, so that the correction is limited to 1.3%, showing that the main sources and sinks of NO_2, i.e., respectively Reactions (3) and (4), approximately balance each other. Losses due to chemistry therefore affect little our measurements of both NO_2 and O_3. These effects are of the same order of magnitude or larger than the long-term drift of the gas analyzers over the time span of the measurements. The concentrations at the output of the cell, and hence the production rates of O_3 and NO_2 (right scales in Fig. 2) can therefore be trusted within typically 10%. On the other hand, the molecule concentrations in the filament volume (left scale in Fig. 2) rely on the estimation of typical filament diameters,[1–4] which may be trusted within a factor of 2. However, the excess of HNO_3 by orders of magnitudes as compared to the amounts required to explain the observed laser-induced water condensation[12] ensures the validity of our qualitative conclusion in spite of this relatively large quantitative uncertainty.

The depletion of NO was estimated by considering the rate $k_3 = 1.9 \times 10^{-14}$ cm^3/s of Reaction (3) (Ref. 17) and the concentration retrieved in the filaments. We find a depletion rate $d[NO]/[NO]dt = k_3 \times [O_3] = 200$ s^{-1}. As a consequence, the NO produced is almost completely oxidized into NO_2 within 50 ms due to the extremely high ozone concentration. This confirms that Reaction (3) is far from being the limiting factor in the generation of HNO_3.

As a conclusion, we have experimentally measured that laser filaments in air generate up to 10^{14}, 3×10^{12}, and 3×10^{13} molecules of O_3, NO, and NO_2, respectively. The corresponding local concentrations in the filament active volume are 10^{16}, 3×10^{14}, and 3×10^{15} cm^{-3} and allow efficient oxidative chemistry of nitrogen, resulting in concentrations of HNO_3 in the parts per million range. The latter forming binary clusters with water, our results provide a plausible pathway for the efficient nucleation observed in laser filaments, especially in subsaturated atmospheres.

We gratefully acknowledge B. Lazarrotto (Service de la Protection de l'Air de Geneve) for supplying the trace gas analyzers. This work was supported by the Swiss NSF (Contract No. 200021-125315).

[1] S. L. Chin, S. A. Hosseini, W. Liu, Q. Luo, F. Theberge, N. Akozbek, A. Becker, V. P. Kandidov, O. G. Kosareva, and H. Schroeder, Can. J. Phys. **83**, 863 (2005).
[2] A. Couairon and A. Mysyrowicz, Phys. Rep. **441**, 47 (2007).
[3] L. Bergé, S. Skupin, R. Nuter, J. Kasparian, and J.-P. Wolf, Rep. Prog. Phys. **70**, 1633 (2007).
[4] J. Kasparian and J.-P. Wolf, Opt. Express **16**, 466 (2008).
[5] P. Béjot, J. Kasparian, S. Henin, V. Loriot, T. Vieillard, E. Hertz, O. Faucher, B. Lavorel, and J.-P. Wolf, Phys. Rev. Lett. **104**, 103903 (2010).
[6] B. La Fontaine, F. Vidal, Z. Jiang, C. Y. Chien, D. Comtois, A. Desparois, T. W. Johnson, J.-C. Kieffer, and H. Pépin, Phys. Plasmas **6**, 1615 (1999).
[7] M. Rodriguez, R. Bourayou, G. Méjean, J. Kasparian, J. Yu, E. Salmon, A. Scholz, B. Stecklum, J. Eislöffel, U. Laux, A. P. Hatzes, R. Sauerbrey, L. Wöste, and J.-P. Wolf, Phys. Rev. E **69**, 036607 (2004).
[8] G. Méjean, J. Kasparian, J. Yu, E. Salmon, S. Frey, J.-P. Wolf, S. Skupin, A. Vinçotte, R. Nuter, S. Champeaux, and L. Bergé, Phys. Rev. E **72**, 026611 (2005).
[9] R. Salamé, N. Lascoux, E. Salmon, J. Kasparian, and J. P. Wolf, Appl. Phys. Lett. **91**, 171106 (2007).
[10] J. Kasparian, M. Rodriguez, G. Méjean, J. Yu, E. Salmon, H. Wille, R. Bourayou, S. Frey, Y.-B. André, A. Mysyrowicz, R. Sauerbrey, J.-P. Wolf, and L. Wöste, Science **301**, 61 (2003).
[11] J. Kasparian, R. Ackermann, Y.-B. André, G. Méchain, G. Méjean, B. Prade, P. Rohwetter, E. Salmon, K. Stelmaszczyk, J. Yu, A. Mysyrowicz, R. Sauerbrey, L. Wöste, and J.-P. Wolf, Opt. Express **16**, 5757 (2008).
[12] P. Rohwetter, J. Kasparian, K. Stelmaszczyk, S. Henin, N. Lascoux, W. M. Nakaema, Y. Petit, M. Queißer, R. Salamé, E. Salmon, Z. Q. Hao, L. Wöste, and J.-P. Wolf, Nat. Photonics **4**, 451 (2010).
[13] W. Byers Brown, Chem. Phys. Lett. **235**, 94 (1995).
[14] V.-M. Kerminen, A. S. Wexler, and S. Potukuchi, J. Geophys. Res. **102**, 3715 (1997).
[15] T. Koop, B. Luo, U. M. Biermann, P. J. Crutzen, and T. Peter, J. Phys. Chem. A **101**, 1117 (1997).
[16] F. Yu, Atmos. Chem. Phys. **6**, 5193 (2006).
[17] J. H. Seinfeld and S. N. Pandis, *Atmospheric Chemistry and Physics—From Air Pollution to Climate Change*, 2nd ed. (Wiley, New York, 2006).
[18] J. Duplissy, M. B. Enghoff, K. L. Aplin, F. Arnold, H. Aufmhoff, M. Avngaard, U. Baltensperger, T. Bondo, R. Bingham, K. Carslaw, J. Curtis, A. David, B. Fastrup, S. Gagné, F. Hahn, R. G. Harrison, B. Kellett, J. Kirkby, M. Kulmala, L. Laakso, A. Laaksonen, E. Lillestol, M. Lockwood, J. Mäkelä, V. Makhmutov, N. D. Marsh, T. Nieminen, A. Onnela, E. Pedersen, J. O. P. Pedersen, J. Polny, U. Reichl, J. H. Seinfeld, M. Sipilä, Y. Stozhkov, F. Stratmann, H. Svensmark, J. Svensmark, R. Veenhof, B. Verheggen, Y. Viisanen, P. E. Wagner, G. Wehrle, E. Weingartner, H. Wex, M. Wilhelmsson, and P. M. Winkler, Atmos. Chem. Phys. **10**, 1635 (2010).
[19] S. Henin, Y. Petit, D. Kiselev, J. Kasparian, and J.-P. Wolf, Appl. Phys. Lett. **95**, 091107 (2009).
[20] G. Fibich and B. Ilan, Phys. Rev. E **67**, 036622 (2003).
[21] I. A. Kossyi, A. Yu. Kostinsky, A. A. Matveyev, and V. P. Silakov, Plasma Sources Sci. Technol. **1**, 207 (1992).
[22] H. L. Xu, A. Azarm, J. Bernhardt, Y. Kamali, and S. L. Chin, Chem. Phys. **360**, 171 (2009).
[23] I. Dotan, P. M. Hierl, R. A. Morris, and A. A. Viggiano, Int. J. Mass Spectrom. Ion Process. **167–168**, 223 (1997).
[24] J. N. Bardsley, J. Phys. B **1**, 365 (1968).
[25] O. V. Braginskiy, A. N. Vasilieva, K. S. Klopovskiy, A. S. Kovalev, D. V. Lopaev, O. V. Proshina, T. V. Rakhimova, and A. T. Rakhimov, J. Phys. D: Appl. Phys. **38**, 3609 (2005).